


ORIGINAL RESEARCH

Decentralised CAVs based on micro–macro flow control (MiMaFC) strategy for multi-intersection traffic network

 Zhengze Zhu^{1,2,4}  | Lounis Adouane³ | Alain Quilliot⁴
¹Institut Pascal, UMR CNRS 6602, Université Clermont Auvergne, Aubière Cedex, France

²Institute of Automotive Engineers, Hubei University of Automotive Technology, Shiyan, China

³Heudiasyc, UMR CNRS 7253, Université de Technologie de Compiègne, Compiègne Cedex, France

⁴LIMOS, UMR CNRS 6158, Université Clermont Auvergne, Aubière Cedex, France
Correspondence

Zhengze Zhu, Institut Pascal, UMR CNRS 6602, Université Clermont Auvergne, 63178 Aubière Cedex, France.

 Email: Zhengze.ZHU@doctorant.uca.fr
Funding information

Project 928, Grant/Award Number: DF928-2020-040; CPER RITMEA, Grant/Award Number: Hauts-de-France region; Investissements d'Avenir, Grant/Award Number: IMoBS3 Laboratory of Excellence ANR-10-LABX-16-01; 2020 Innovative Development of the Industrial Internet, Grant/Award Numbers: TC200H033, TC200H01F

Abstract

Advanced intersection control systems have been created to alleviate traffic congestion. CAVs may benefit from cooperative navigation in order to address the regular traffic issue. Due to whole uncertainty in transportation network, the conventional motion planning for local areas may lead to undesirable effects in long run. In prior works, a micro–macro flow control (MiMaFC) strategy is used to investigate CAVs' navigation at unsignalised intersections by taking flow velocity and vehicle passing priority into account. To get a better understanding of motion control and how it can be utilised to impact traffic flow behaviour, this study expands the intersection navigation protocol and develops a velocity planning methodology based on the proposed MiMaFC technology. Correspondingly, cooperative navigation protocol used in the addressed architecture is specifically developed for CAVs that continually cross intersections. Further, spatio-temporal velocity adaption mechanism is presented in this work. Depending on the vehicles' location and speed, CAVs might use either the MiMaFC-based or self-interested velocity strategy. Simulation results, which include a congested traffic network, are shown to demonstrate the proposed method's potential. The study found that the suggested motion planning framework may increase urban network mobility over a non-supervised CAVs system.

1 | INTRODUCTION

Urban transport systems are expected to be enormously improved thanks to the Connected and autonomous/automated vehicles (CAVs) [1, 2]. CAVs may contribute in a better manner to boost the public transportation in urban areas and regulate their navigation in an arranged way [3, 4]. From this perspective, an important question arises: how can CAVs help to fulfil the increasing mobility demands and better adapt intelligent transportation development in the future? In fact, a CAVs system is supposed to engage in cooperative navigation tasks [5]. The majority of studies indicate that CAVs will become a reality in the near future (although at very modest market penetration rates) and will have the capacity to significantly decrease traffic congestion, road accidents, and car emissions [6–8]. Additionally, intersections may

be instrumented to broadcast messages to neighbouring cars through DSRC or C-V2X, which contains information about the signal phase, time and geometry of the intersection [1]. Due to advancements in both the on-board system and sophisticated sensors in surrounding environments, research under the premise of all CAVs on the road has also attracted the traffic control community's attention [1, 9, 10].

Numerous control architectures for CAVs systems are described in the literature [3, 5]. The precise classifications addressed some of the specifics of the multi-vehicle control systems used: centralised vs. decentralised control approach [11]. A centralised control method for CAVs is explored in [12], with the purpose of minimising a cost function that incorporates CAV safety, efficiency, and ride comfort. The research in ref. [13] established a decentralised theoretical framework for CAVs coordination. In this study, rear-end, speed-dependent

This is an open access article under the terms of the [Creative Commons Attribution-NonCommercial License](https://creativecommons.org/licenses/by-nc/4.0/), which permits use, distribution and reproduction in any medium, provided the original work is properly cited and is not used for commercial purposes.

© 2022 The Authors. *IET Intelligent Transport Systems* published by John Wiley & Sons Ltd on behalf of The Institution of Engineering and Technology.

safety constraints were explored. Other studies with similar discussion in various control approach/architecture might also be discovered in refs. [14–17]. Because maximising the flexibility and autonomy of controlled CAVs is often preferred. Thus, some of the above-mentioned literature extensively research decentralised multi-vehicle control systems in complex environments or situations (mainly in terms of cooperative scheduling, planning and control in highway entrance/exit ramps or intersection/roundabout coordination). Additionally, CAVs for intersection management have emerged as a prominent research field for the use of cooperative technology inside the discussed control framework.

Indeed, the research work related to intersection management has gained considerable attention during the last decade. Interesting and comprehensive surveys in relation with this issue are reported in refs. [2, 18–21]. Several signal-based control systems assured the efficient management of intersections and aided in the alleviation of traffic congestion [21, 22]. Thanks to the new emergent vehicular communication technologies, a large range of unsignalised intersection management approaches are also introduced in recent literature [23, 24]. It provides promise for cooperative intersection control, particularly in terms of adapting to the use of CAVs. Additionally, those cooperative intersection control methods can be classified into: cooperative resource reservation techniques, trajectory planning approaches and virtual traffic lights solutions [18]. Our previous works [25–27] also addressed a trajectory planning-based method for cooperative navigation at a signal-free intersection. The CAVs system's global goal is challenging: to provide compelling advantages to the system as a whole. Additionally, cooperative motion planning is critical for adapting the whole traffic environment, given the fact that it is preferred to develop control approaches from a system perspective. Therefore, there is still a need to develop cooperative navigation techniques in complex intersection networks in urban environments.

1.1 | Related work

Most urban road users feel that implementing CAVs technologies (such as cooperative trajectory prediction and motion planning) will considerably increase urban road capacity at a corridor or a road network level in a fully automated setting [28]. In this sense, these CAVs applications blur the line between traffic management and multi-vehicle coordination [1]. Essentially, it addresses comparable issues at the road network level rather than at the vehicle level. For concerned readers, refs. [22, 29, 30] provide an overview of traffic control, and refs. [21, 22, 31] discuss the link between traffic control and vehicle connectivity. The existing CAVs-based control algorithm is mainly concerned with single intersection. Cooperative driving at neighbored intersections has also been studied by researchers in ref. [32]. However, multi-vehicle navigation has gotten less attention for urban traffic management with network-wide traffic control issues [21]. The primary tasks or difficulties that distinguish the control technique for isolated

intersections from corridors or network-level control can be divided into two major issues: coordination of multiple intersections using CAVs to improve traffic flow in road networks, and accurate traffic prediction/estimation techniques. The following explores the unsignalised CAVs-based urban traffic control at multiple intersections: in ref. [33], a tile-based reservation system is expanded to control a network of linked intersections by using the typical multi-agent systems (driver agent, intersection manager). In this method, an autonomous intersection management (AIM) system was created to reserve a conflict-free path and determine if a vehicle's crossing request should be granted. Additional study conducted in ref. [34] is aimed to investigate the potential of incorporating dynamic traffic assignment (macroscopic level) into the proposed AIM-based intersection control system (microscopic level). The primary distinctions between different AIM-based traffic control methods are the controlling mechanism or navigation policies [35]. Most AIM-based studies can be simulated successfully. However, it is highly dependent on the decision-making of the intersection manager. Further, vehicle negotiation systems were proposed as a decentralised solution to deal with multiple intersections control. In a negotiation-based approach (sometimes called auction-based approach [36]), the intersection manager is removed. The agents of the vehicles interact between them to decide the order of passage and departure from the intersection. Specifically, vehicles in the collective negotiating system are intended to solve an optimisation problem using sensed vehicle data (location, speed, and inter-distance etc.). The negotiated results may include information on when and how fast to merge [37]. However, the technique is limited by the number of vehicles attempting to negotiate. Just a few vehicles near the intersection are considered to make decisions within a certain time interval. Negotiation-based control often performs less well than AIM-based control, but the vehicle negotiation system in the valuation-aware mechanism [36] has a lower overhead for making decisions and generating agile responses to any unexpected changes [22]. In particular, many decentralised approaches for CAVs cooperative navigation still requires a local manage agent in charge of synchronising the vehicle to cross the intersection [35]. It is important to note that the dynamics and distributed controller are qualities of the individual CAV, but the information flow network and macro traffic control are aspects of the entire CAVs system. Consequently, most of the research on on-ramp/intersection coordination in road networks use a multi-layer/multi-level control framework [35, 38]. In previous work [39, 40], we proposed a multi-layer hybrid control policy and motion planning (MHCP-MP) framework for hierarchical control of CAVs cooperative navigation at multiple intersections. A micro–macro flow control (MiMaFC) approach is proposed in the introduced macroscopic management layer to explain the CAV's global navigation performance in terms of overall traffic mobility. The MiMaFC approach incorporates the aggregated speeds (a harmonised flow speed proportional to the traffic density) of the downstream as well as the associated road weights proportionate to the upstream density. To solve intersection management without traffic lights, a decentralised optimisation control based on the MiMaFC technique has been deployed

in ref. [40]. CAVs systems have the ability to increase traffic efficiency at crowded intersections by using MiMaFC-based motion planning with the goal of ensuring safe and fast driving. We also developed an appropriate protocol for ego-vehicle to execute its optimisation procedures with other vehicles.

In summary, there are two main challenges that need to be addressed in the context of CAVs cooperative navigation in a complex intersection network (non-highway scenarios). First, how to create a specialised large-scale optimisation framework for addressing the issue of large-scale vehicle operation. Due to the fact that unexpected driver behaviours often contribute to traffic uncertainty, vehicles are prone to unnecessary delay and, as a result, slow traffic [41]. Additionally, increased traffic data must be analysed inside a CAVs system. There is no established concept, standard or platform for resolving this problem at the moment. Rather than that, a framework that unifies the protocol for cooperative navigation. Second, we are concerned not only with the safe movement of a single agent inside CAVs, but also with the coordinated and safe movement of the whole system. Nonetheless, in the expanded macro traffic flow model, the cooperative motion planning methods remain inexact and suboptimal. Additionally, the trajectory chosen to resolve conflicts in a local region may result in an increase in travel time and fuel consumption over time. As a result, speed guidance (at a targeted vehicle speed or a constrained speed) is required to account for macro-traffic circumstances.

1.2 | Contributions and organisation

In order to bridge the gap, the MHCP-MP framework was further developed based on our prior works [39, 40]. In fact, the prior research tended to categorise all vehicles as collaborative agents for system optimisation in congested traffic. The computation load for repeated system optimisation is high, and obtaining a feasible solution is challenging. Because CAVs are sensitive to the spatio-temporal circumstances for picking a successful strategy, it is targeted in the proposed work is to thoroughly study these aspects, which were not addressed in our prior work. In this research, we constructed a refined intersection management system to address these issues. The following is a summary of the main contributions:

- The MHCP-MP framework is enhanced with an intersection navigation protocol for CAVs that traverse intersections continually under decentralised control. The protocol is implemented using a local supervisor (at the management layer) capable of assuring an effective collaboration policy to maintain a congested-free network. In addition, a region division at an intersection is proposed for CAVs decision-making that enables cars to get a feasible solution without labelling all agents involved in the optimisation process.
- This work introduces a spatio-temporal velocity adaption mechanism: CAVs were permitted to employ either the MiMaFC-based [39, 40] or self-interested speed strategy [25], depending on their present position and speed. The

numerical solution set of the MiMaFC-based strategy is given in this paper. Vehicles operating under this mechanism may ensure optimal/suboptimal performance in accordance with hybrid MiMaFC policies in the MHCP-MP framework. It lessens the complexity by allowing for more cars at the merging zone of an intersection.

In comparison to previous works [39, 40], this study aimed to provide an enhanced navigation protocol/diagram under the assumed MHCP-MP framework, considering cooperating agents, traffic conditions, and more precise deployment of motion planning inside an urban intersection network. Remarkably, the decision-making process is repeated throughout the whole intersection management, and it is difficult to negotiate in a system of high complexity. In this paper, the navigation protocol/diagram provided by a local supervisor ensures that a vehicle may pick the appropriate approach based on the region's division of intersections. Thus, the vehicle might receive an adaptive strategy that reduces the computation requirements of the re-planning phase. In addition, quadratic programming is used to show how the spatio-temporal velocity adaptation strategy can be used to find the numerical solution of the suggested MiMaFC-based velocity strategy. These were not done in the previous work. The remaining of this paper is organised as follows: Section 2 details the studied problem while introducing the overall proposed MHCP-MP framework. Section 3 presents the proposed macroscopic flow model. Section 4 discussed a technique for safe and efficient intersection navigation protocol that incorporates spatio-temporal velocity adaptation. The suggested MiMaFC velocity strategy set's numerical solutions are also introduced. Section 5 performs and interprets the obtained simulation results. The paper contributions and future work are summarised in Section 6.

2 | TRAFFIC FRAMEWORK: MHCP-MP

The overview of the addressed circumstances is explained in Figure 1. It is considered in this work that all the navigating vehicles have the possibility to interactive with them and with the infrastructure through communication. The designated paths of CAVs have been computed based on the stationary global information for each vehicle. A module named local supervisor (S_{Loc_A}) is located at each intersection region. Additionally, assume that downstream traffic information (see Figure 1) are provided by roadside sensors implanted along the mid-blocks between two intersections. For the sake of simplicity, a S_{Loc_A} is assumed to receive updated approaching traffic flow data without considering measurement errors (and/or delays) induced from the infrastructure-to-infrastructure (I2I) communication.

The proposed two-layer MHCP-MP framework is shown in Figure 2. The MHCP-MP architecture is divided into two primary layers for each intersection: a macroscopic flow model (cf. Section 3) and a microscopic autonomous intersection management (AIM) model (cf. Section 4). Local supervisors S_{Loc_A} observe the downstream traffic flow status. Thus, the traffic aggregated speeds and the rights of passage are then

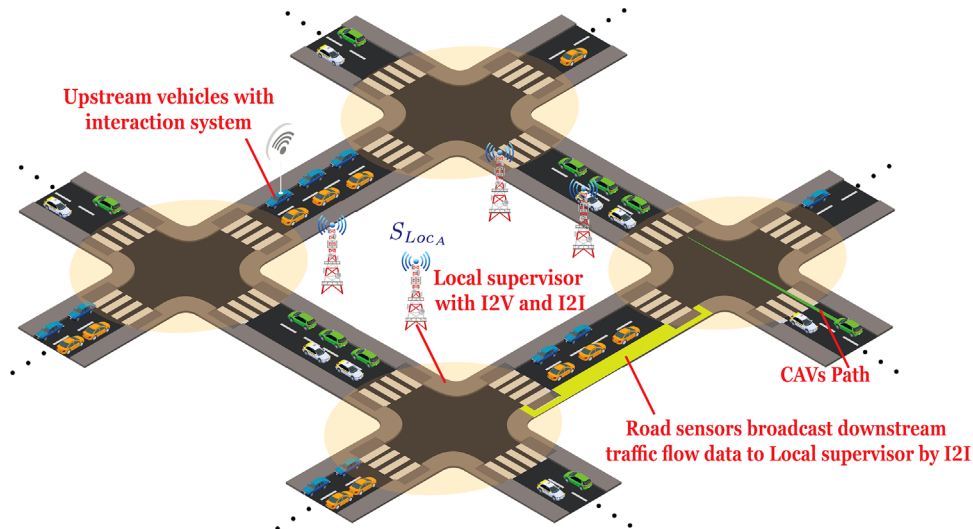


FIGURE 1 Urban road network for autonomous vehicle cooperative navigation with local supervisor S_{Loc_A} at each intersection region

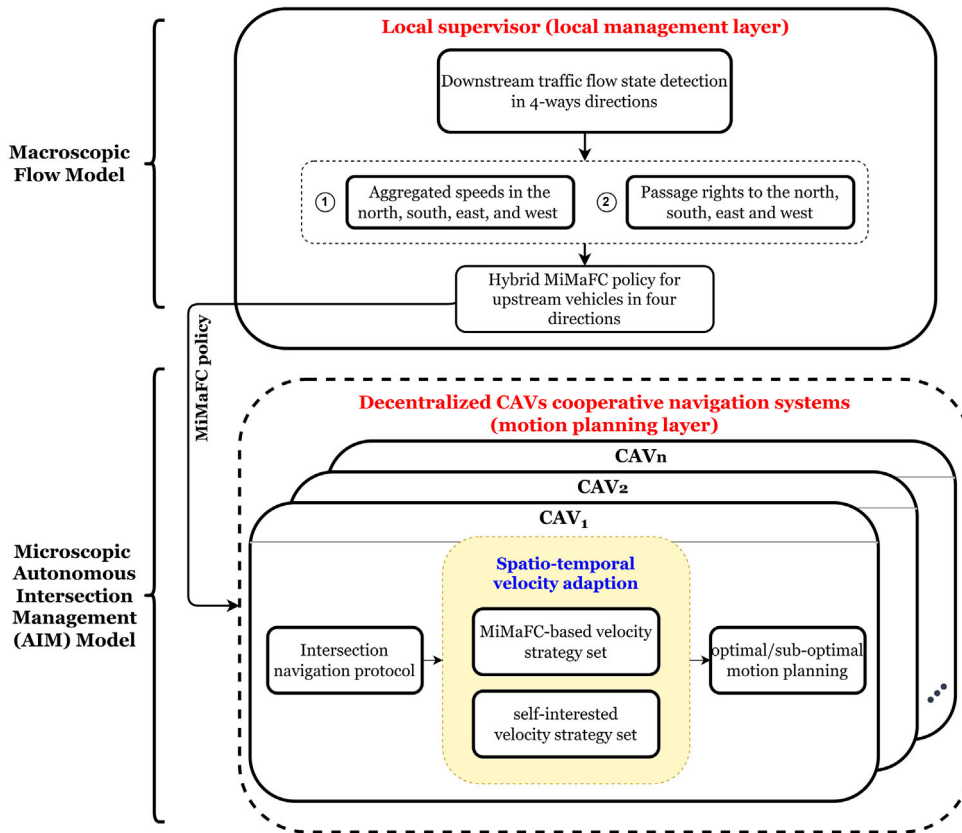


FIGURE 2 Basic schematic of the proposed multi-layer hybrid control policy and motion planning (MHCP-MP) framework

disseminated for upstream vehicles¹ in different directions. CAVs are therefore considered to have on-board system to retrieve a hybrid MiMaFC policy from S_{Loc_A} . It is important to note that all the approaching CAVs in the four-way

upstream are treated as a decentralised cooperative system, which individual vehicle could make decision by themselves. The management layer's local supervisors S_{Loc_A} transmit only instructions/rules (i.e. MiMaFC policy, see Figure 2) for inter-vehicle coordination. CAVs are expected to follow the recommended navigation protocol and generate the velocity

¹ Vehicles that will cross imminently the intersection (cf. Figure 1).

set utilising a spatio-temporal velocity adaption mechanism in the AIM model. Finally, an optimal control algorithm is used to determine the optimal/suboptimal speed at which the vehicle should transit the intersection.

3 | MACROSCOPIC FLOW MODEL

The macroscopic flow model interprets the real-time state of the dynamic transportation network including multiple intersections. Firstly, a primitive car-following model is illustrated by kinematic equations like the following:

$$\begin{cases} a_i(t) = u_i(t) + \varepsilon_i(t) \\ v_i(t + \Delta t) = v_i(t) + a_i(t) \times \Delta t \\ x_i(t + \Delta t) = x_i(t) + v_i(t) \times \Delta t + \frac{1}{2} a_i(t) \times \Delta t^2 \end{cases} \quad (1)$$

Where $x_i(t)$ and $v_i(t)$ denote respectively the displacement and velocity of the vehicle i at time instant t . $a_i(t)$ is the corresponding acceleration for a time interval Δt . Besides, $a_i(t)$ in Equation (1) is addressed by the control input $u_i(t)$ and an uncertain disturbance factor $\varepsilon_i(t)$ which is related to the perception and sensing errors. It is supposed that $u_i(t)$ corresponds to a movement of a particle with constant acceleration between two instants, which has been defined by Δt . Thus, considering the relative distance $\Delta x_{i,i-1}(t) = x_{i-1}(t) - x_i(t)$ and relative speed $\Delta v_{i,i-1}(t)$ between two successive vehicles (i.e. ego vehicle i and vehicle $i-1$ ahead). It assumes that CAVs either perform cruise control (for free motion) to maintain a preset speed v_{ref} or adaptive cruise control (ACC) when a vehicle ahead is detected within a distance $\Delta x_{i,i-1}(t) \leq R_w$. R_w is assumed to be a fixed sensing range. A reference distance $d_{\text{ref}}(t)$ is defined as:

$$d_{\text{ref}}(t) = d_{\text{safe}} + \Delta x_{i,i-1}^* \quad (2)$$

In Equation (2), d_{safe} is the preset standstill safe distance. $\Delta x_{i,i-1}^*$ is the desired distance at current speed. Thus, the control law $u_i(t)$ for vehicle i can be addressed in Equation (3):

$$u_i(t) = \begin{cases} -k_0 \cdot (v_i(t) - v_{\text{ref}}) & \text{if } \Delta x_{i,i-1}(t) > R_w \\ k_1 \cdot (\Delta x_{i,i-1}(t) - d_{\text{ref}}(t)) + k_2 \cdot \Delta v_{i,i-1}(t) & \text{others} \end{cases} \quad (3)$$

Where $\{k_0, k_1, k_2\}$ are positive control gains. It is important to remark that $\Delta x_{i,i-1}^*$ represents the preferred distance for each vehicle in Equation (2). CAVs can be assigned with stochastic space policy like human driver applying invasive or conservative following strategy on road. In this paper, the desired distance $\Delta x_{i,i-1}^*$ is defined by the stochastic time headway tb_i : $\Delta x_{i,i-1}^* = tb_i \cdot v_i(t)$. Further, it is assumed that $tb_i = \hat{tb}_i$ is sampled based on a shifted log-normal distribution [42]: $\hat{tb}_i \sim \log\text{-}N(\mu_{\nu}, \sigma_{\nu})$.

Next, the urban road network is further explained in this study. We will consider an area of nine neighbourhood intersec-

tions which are combined together as an urban road network like in Figure 3. The whole transportation network contains 48 links and nine intersections. The origins and destinations (O-D) are set to manage the flows input/output at the borders of the traffic network. Clearly, destinations points are located in 12 links (thus, define the destination links number: $n_D = 12$) which are not belong to any of the internal intersection areas (red lines in Figure 3). Further, it is assumed that the traffic load is homogeneously distributed without considering external changes.

In addition, the traffic flow characteristics linking flow, speed and density can be uniformly defined and revealed by macroscopic fundamental diagram (MFD) [43–45]. There are many ways to interpret the value of fundamental traffic flow characteristics (flow, speed and density). Here, the measured space mean speed V , traffic density K , and calculated travel flow Q are addressed in this paper (see Figure 3 for example). Generally, we consider in the proposed modelling that the infrastructure has the possibility to cyclically collect instantaneous vehicle speed v_i and vehicle number N_i for each lane. Thus, the lane density at every instant can be defined as follows:

$$K_{L_i} = \frac{N_i}{\text{LGTH}_i}, \quad K_{D_i} = \frac{N_{d_i}}{\text{LGTH}_i} \quad (4)$$

Where LGTH_i is the length of a link, K_{L_i} represents the lane's density towards the intersection (black arrows in Figure 3) and K_{D_i} is the destination lane's density (red arrows in Figure 3, N_{d_i} is the vehicle number in destination lane). Accordingly, the density of intersection K_{S_i} (combined by n_{L_i} links, for instance, a group of $n_{L_i} = 4$ yellow arrows in Figure 3) is defined as:

$$K_{S_i} = \left(\sum_{L_j=1}^{n_{L_i}} K_{L_j} \right) / n_{L_i} \quad (5)$$

Moreover, the overall intersections density K_S and exits lane density K_D are developed as follows (n_S and n_D are respectively the overall number of intersections and the number of destinations):

$$\begin{cases} K_S = \left(\sum_{S_j=1}^{n_S} K_{S_j} \right) / n_S \\ K_D = \left(\sum_{D_j=1}^{n_D} K_{D_j} \right) / n_D \end{cases} \quad (6)$$

The space-mean speed² has been more commonly adopted to reveal current traffic state than time-mean speed³ (which overestimates the influence of faster vehicles [46, 47]). Hence, the space-mean speed, which is also calculated as a harmonic mean of collected vehicle speeds, is used in this study as the traffic

² The space-mean speed is the average speed of vehicles travelling a given segment of roadway during a specified period of time and is calculated using the average travel time and length for the roadway segment (i.e. Space mean speed = $\frac{\text{distance travelled}}{\text{avg. travel time}}$ as seen in ref. [46], Chapter 1).

³ The time-mean speed is defined by the arithmetic average speed of all vehicles for a certain duration of time.

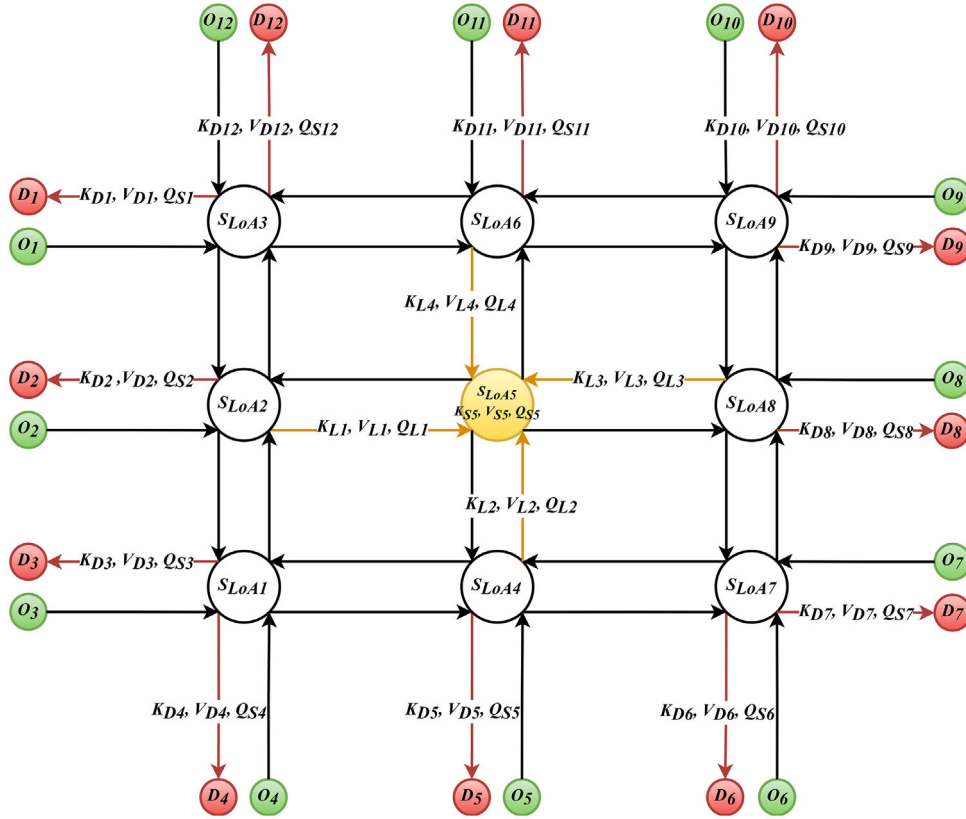


FIGURE 3 CAVs navigation in transportation network with multiple unsignalised intersections: the origins (destinations) are noted by $O_i(D_i)$. Each four-way intersection is in charged by a local supervisor S_{LoA_i} . The 3-tuple of traffic density, velocity and flow rate are defined for each link $\{K_{L_i}, V_{L_i}, Q_{L_i}\}$, destination lane $\{K_{D_i}, V_{D_i}, Q_{D_i}\}$ and intersection area $\{K_{S_i}, V_{S_i}, Q_{S_i}\}$

velocity associated with a specified length of roadway. Thus, the traffic velocity for flow input lane, exit lane and intersection area are respectively defined as $\{V_{L_i}, V_{D_i}, V_{S_i}\}$, see Equation (7):

$$\begin{cases} V_{L_i} = N_i / \sum_{i=1}^{N_i} (1/v_i) \\ V_{D_i} = N_{D_i} / \sum_{i=1}^{N_{D_i}} (1/v_i) \\ V_{S_i} = N_{S_i} / \sum_{i=1}^{N_{S_i}} (1/v_i) \end{cases} \quad (7)$$

Where $\{N_i, N_{D_i}, N_{S_i}\}$ are the vehicle quantity in the corresponding areas. Similarly, the traffic velocity for destination lanes (for N_D vehicles) and overall intersections (contain N_S vehicles) are written as:

$$\begin{cases} V_D = N_D / \sum_{i=1}^{N_D} (1/v_i) \\ V_S = N_S / \sum_{i=1}^{N_S} (1/v_i) \end{cases} \quad (8)$$

In such a manner, the calculated flow rate can be also addressed as $Q_{L_i} = K_{L_i} \times V_{L_i}$ (for every links), $Q_{D_i} = K_{D_i} \times V_{D_i}$ (for destination lanes) and $Q_{S_i} = K_{S_i} \times V_{S_i}$ (for an intersection area) at every instant (see also in Figure 3). In so doing, we avoid to hourly measure flow rate which reflect the equal

traffic knowledge as calculated flow rate in the experimental intersection network. Next, the obtained traffic key factors are formulated by the notable Greenshields model [48] for every single lane as follows:

$$\begin{cases} V_{L_i} = V_f \left(1 - \frac{K_{L_i}}{K_{jam}} \right) \\ Q_{L_i} = V_f \left(K_{L_i} - \frac{K_{L_i}^2}{K_{jam}} \right) \end{cases} \quad (9)$$

where V_f and K_{jam} are respectively the free-flow speed (maximum desired speed) and jam density (where automobiles are unable to move) regarding a predefined traffic fundamental diagram. Thus, $[V_{L_i}, Q_{L_i}]$ are the dependents on the measured lane density K_{L_i} . It is worth acknowledge that if the vehicle number increasing consistently (while $\partial Q_i / \partial K_{L_i} \leq 0$) till to the maximum road capacity, the flow rate will decrease and even collapse to zero at the jam density K_{jam} .

Ultimately, CAVs are supposed to adopt appropriated actions at intersection areas w.r.t. the MiMaFC policy info from the local supervisor as depicted in Figure 2. The MiMaFC policy includes the aggregate speed (flow speed) V_{L_i} of the downstream lane referring to Equation (9), as well as the accompanying road weights W_{r_i} proportional to

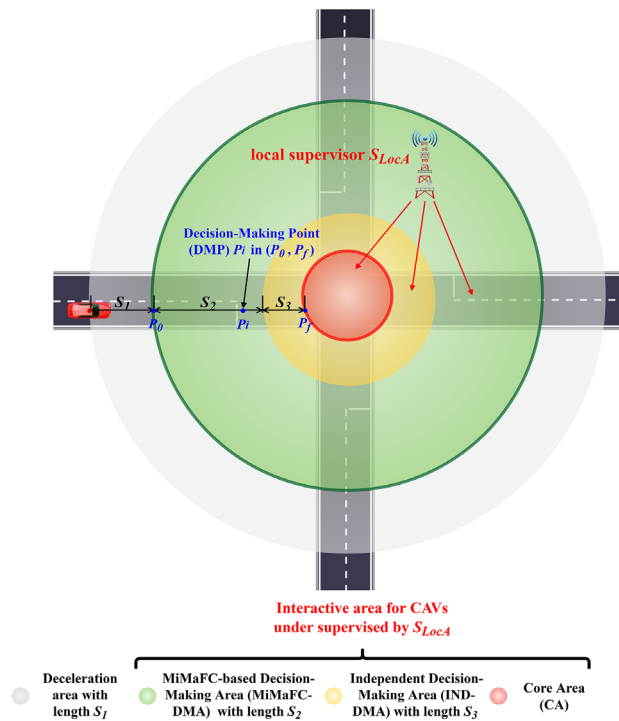


FIGURE 4 Individual vehicles approach the intersection and make decision from P_0 to participate in cooperative navigation. The interactive area supervised by S_{LocA} is divided into three parts (i.e. MiMaFC-DMA, IND-DMA, and CA identified by different colours), each of which implements different corresponding navigation protocol for cooperative strategy

upstream density. In addition, W_{r_i} is determined by variable $\partial Q_i / \partial K_{L_i}$ to avoid congested situation from authors' previous work [39, 40]). Finally, critical MiMaFC policy information, namely $[(\forall_{L_1} W_{r_1}), (\forall_{L_2} W_{r_2}), (\forall_{L_3} W_{r_3}), (\forall_{L_4} W_{r_4})]$ for example, is assigned to an incoming vehicle within an four-way intersection's borders.

4 | MICROSCOPIC AIM MODEL

The microscopic AIM model is divided into two succeeding parts to highlight the proposed intersection navigation protocol (cf. subsection 4.1) and spatio-temporal velocity adaption mechanism (cf. subsection 4.2) in this paper.

4.1 | Intersection navigation protocol

As seen in Figure 4, before reaching the initial decision-making point P_0 , a car approaching the intersection will decelerate at a specific distance S_1 (e.g. $S_1 = 50$ m which corresponds to the bounds of local interactive area). When a vehicle arrives at P_0 , a local supervisor S_{LocA} (cf. Figure 4) immediately sends the local MiMaFC policy, which instructs the vehicle's cooperative motion planning. Particularly, if two or more cars join P_0 (from different directions) at the same time, a local supervisor S_{LocA} will appoint the vehicle that makes the decision first at random.

The interactive area is divided into three parts labelled by different colours in Figure 4. If a vehicle is identified as a cooperative agent, it will firstly create the MiMaFC-based speed strategy set (cf. subsection 4.2.1) which gain the most chance to satisfy the S_{LocA} policy. Unfortunately, the crossing strategy is sensitive to the initial speed and it may be re-planned in the proposed cooperation protocol as mentioned in the following paragraph. Thus, MiMaFC-based decision-making area (MiMaFC-DMA, the green part in Figure 4) is reserved with a length S_2 for vehicles to find the best-sampled strategy set to find a feasible cooperative trajectory at other DMP P_i (as seen in Figure 4). Secondly, when a vehicle still cannot find a feasible solution to satisfy the local policy (or have to recompute a solution for cooperative navigation) after MiMaFC-DMA, it will adopt the self-interested strategy set (cf. subsection 4.2.1) in the independent decision-making area (IND-DMA, the yellow area in Figure 4). In so doing, safety solution can be lastly guaranteed when a vehicle closing to the intersection core area (CA) with red colour in Figure 4. In such a case, the S_{LocA} policy cannot be fully satisfied. But the vehicle's priority (road weights) are still considered in the optimised trajectory. Thirdly, after the final decision-making point P_f (see Figure 4), vehicles in CA are not permitted to modify the targeted speed profile. It is crucial to note that the proposed assumptions and protocols are primarily designed for the vehicle's decision-making layer within a predicted time horizon. However, it is conceivable for our proposed cooperative navigation technologies to be compatible with a control layer in order to cope with more complex real-world dynamics. In the following subsections, we will further describe the primary components addressed in the proposed intersection navigation protocol.

4.1.1 | Vehicle sorting

Firstly, a new car added in the CAVs system executes sorting algorithm (cf. Algorithm 1) to identify the interactive vehicles. The cooperative vehicles need to further choose their intersection strategies set. Notably, the preceding entering vehicle that owns the assigned crossing strategy usually does not cooperate with a new arriving vehicle until there is a conflict that cannot be avoided by the succeeding cars' own efforts. Particularly, vehicle sorting occurs regularly (at a short interval, for instance 0.1 s) in all interactive areas for CAVs supervised by S_{LocA} .

A sorting algorithm (as shown in Algorithm 1) is firstly performed to identify the interactive vehicles at P_0 (see Figure 4). Let us assume that the embedded motion planner of each vehicle in the distributed CAVs system SYS can update the coordination state at every instant. Then, the Boolean's values are correctly assigned for the labelled states such as: collaboration flag V_{Col} , optimisation flag V_{opt} , conflict flag $V_{conflict}$ and remain in intersections flag V_{rem} etc. When a vehicle equipped with an embedded system enters a local monitored area, it will initialise all of these default flags (at P_0). The detailed steps to distinguish between the collaborative and non-collaborative vehicles are given in Algorithm 1.

ALGORITHM 1 Sorting algorithm for collaboration

```

/* The sorting algorithm is executed
periodically in the supervised areas
*/
Input:  $SYS, V_{opt}, V_{conflict}$  and  $V_{rem}$ 
Output:  $V_{Col}$ 
/* Initial  $V_{opt}, V_{conflict}, V_{rem}, V_{Col}, AHD_{conflict}$  are
set to the default value 0 */
1 if vehicle in local area then
2   for all  $i \in SYS$  do
3     if  $V_{opt} == 0$  then
4        $V_{Col} = true$ ; // The vehicle without
optimal strategy should
participate in collaboration
5       if  $AHD_{conflict} == 1$  then
6          $V_{Col} = false$ ; // The ahead vehicle
fails to find any solution
7     else
8        $V_{Col} = false$ ;
9       if  $V_{conflict} == 1$  then
10         $V_{Col} = true$ ; // The vehicle
participates in collaboration
when an inefficient strategy
induced conflict
11      if  $V_{rem} == 1$  then
12         $V_{Col} = true$ ; // The vehicle
participates in collaboration
when it stays at the local
area after predicted time.
13 else
14    $V_{Col} = false$ 
15 return  $V_{Col}$ ;

```

4.1.2 | Risk valuating

Secondly, the collaborative vehicle calculates its minimum time-to-collision (TTC) which is a risk indicator to describe the remaining time for a probable collision between any two vehicles [49, 50]. The developed 2D TTC in our prior work [27] (this article focuses on developing risk-sensitive intersection cooperation strategies) is revisited to identify the cars that have potential conflicts with other vehicles. Noting that, a threshold of TTC_{min} is used to select the violated 2D TTC. A vehicle that does not hit the minimum threshold TTC_{min} will execute a constant accelerating strategy by predefined a_{ref} (if it is the only vehicle) or maintain current speed (if there are other vehicles). Notably, the risk valuating mechanism that is first implemented at P_0 is capable of handling a trivial situation (e.g. not too many automobiles in an interaction) without requiring additional optimisation. Additionally, it is conducted on a frequent basis to monitor the collision risk in all local regions.

4.1.3 | Spatio-temporal velocity adaption

The CAVs system necessitates a deliberate effort on velocity planning while including the local supervisor's policy or ego, a process known as spatio-temporal velocity adaption. Par-

ticularly, the labelled cooperative agent (i.e. $V_{Col} = true$ after Algorithm 1) will run an optimisation algorithm which is impacted by the aforementioned MiMaFC-based speed strategy set from S_{Loc_4} in MiMaFC-DMA with length S_2 (green part in Figure 4). The aggregated speed and lane priority are both considered among a utility maximising model (cf. subsection 4.2.1). The feasible solution within a time horizon $T_{horizon}$ will be adopted for the vehicle's control system. In addition, if a vehicle does not find any solution in former step, it will decelerate to find a better-sampled strategy set in the next time instant during it is driving in S_2 . Further the detected conflict vehicles are permitted to do cooperative multi-agent optimisation immediately, if they are both out of the CA. The MiMaFC strategy set from S_{Loc_4} is still adopted in the cooperation. However, if cooperative vehicles are placed in IND-DMA with length S_3 (which is typically characterised as being shorter than S_2 and closer to CA; see the yellow region in Figure 4), they will solely follow their own self-interest strategy set regardless of the local aggregated speed policy. In such an IND-DMA of length S_3 , it is assumed to prioritise a safe intersection crossing before P_f (as seen also in Figure 4). Finally, vehicles will either discover an admissible solution to avoid any conflicts (before P_f) or decelerate to wait a chance to find better sampled-strategy set at next DMP P_i belong to MiMaFC-DMA or IND-DMA (as seen in Figure 4).

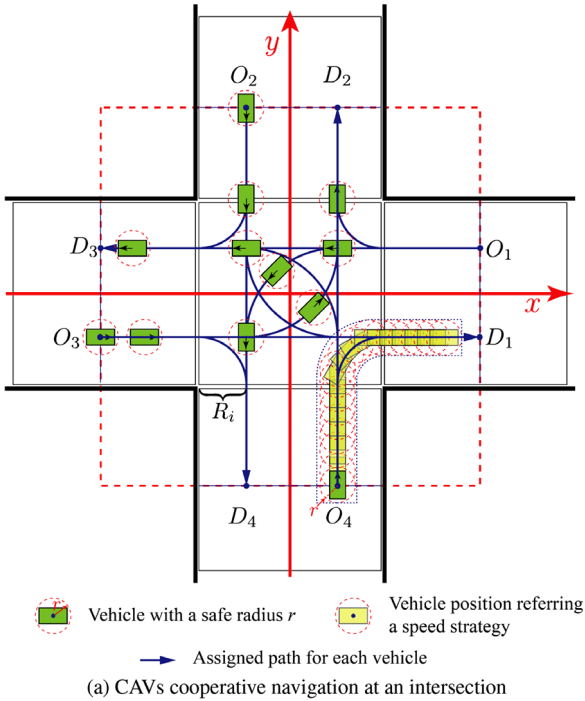
In summary, the intersection navigation protocol described in this paper ensures the safe and optimal/suboptimal operation of subsequent vehicles by allowing them to make decisions using the spatio-temporal velocity adaption mechanism. As a consequence, the next section details the analytical procedure for generating the collection of velocity strategies set.

4.2 | Velocity planning-based CAVs cooperation

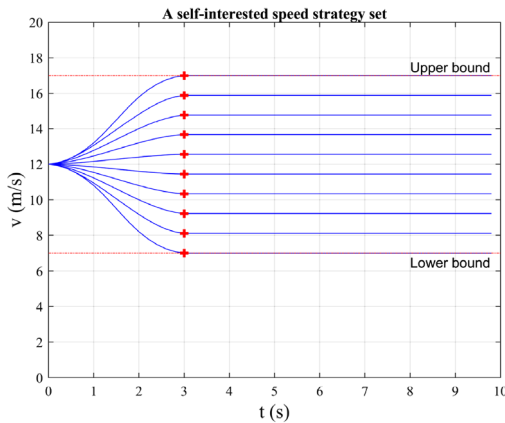
In this section, the aforementioned MiMaFC-based strategy set and self-interested strategy set will be further developed inside the multiple vehicles cooperative optimisation process (cf. subsection 4.2.1). The numerical solutions for MiMaFC-based velocity set is given in subsection 4.2.2).

4.2.1 | Velocity sets for optimisation

The conflict resolutions were developed with the aim of producing a low-complexity and rapid optimisation strategy for crossing intersection. In fact, the vehicle's path is supposed to be fixed during the movement in the local area. As shown in Figure 5(a), the geometry of the 2D road path is either straights (like $O_4 \rightarrow D_2$) or two lines with a tangent quarter circle at a corner (like $O_4 \rightarrow D_1$). Consider $(X_{O_i, D_j}^i, Y_{O_i, D_j}^i)$ to be the x - y coordinates along $O_i D_j$. $(X_{R_l}^i, Y_{R_l}^i), (X_{R_r}^i, Y_{R_r}^i)$ represents the left and right coordinates of the circle centre. R_i is the minimum radius of a quarter circle (cf. Figure 5(a), consequently, the intersection width is $4R_i$). The vehicle 2D path (x, y) may thus be



(a) CAVs cooperative navigation at an intersection



(b) A self-interested speed strategy set

FIGURE 5 An illustration of the possible CAVs trajectories with sampled self-interested speed profiles

described as Equation (10):

$$\begin{cases} x = X_{R_i}^i + 3R_i \cos \theta, y = Y_{R_i}^i + 3R_i \sin \theta, \theta \in [0, \frac{\pi}{2}] \text{ left turn} \\ x = X_{R_r}^i - R_i \cos \theta, y = Y_{R_r}^i + R_i \sin \theta, \theta \in [\frac{\pi}{2}, \pi] \text{ right turn} \\ x = X_{O_i, D_j}^i \text{ or } y = Y_{O_i, D_j}^i \text{ if others} \end{cases} \quad (10)$$

Therefore, the only degree of freedom to re-plan a conflict-free trajectory is the speed for each of the collaborative agents. As seen in Figure 5(a), the vehicles (e.g. the green rectangles) are assigned paths (e.g. the blue arrow) with origins O_i and destination D_j before crossing the intersection. For simplify, a red circle of radius r is defined to surround the car during movement. Any two circles in the 2D graph cannot violate a centre

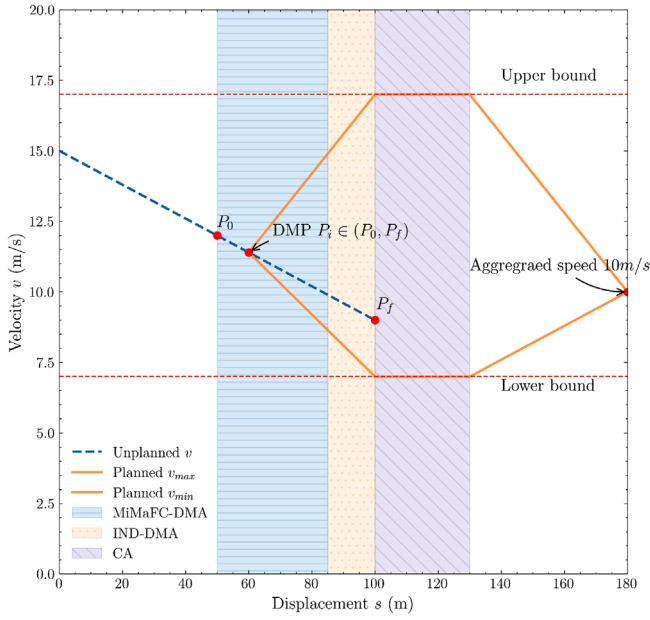
distance less than $2r$ when a vehicle follows its path. Therefore, a velocity planning-based optimisation problem for CAVs is formulated in this paper. Particularly, the formulated model only uses the information of the displacements in the path without concerning the path geometry. In so doing, the algorithm is also independent of the topology of the intersection as long as the possible paths are defined.

Self-interested speed strategy:

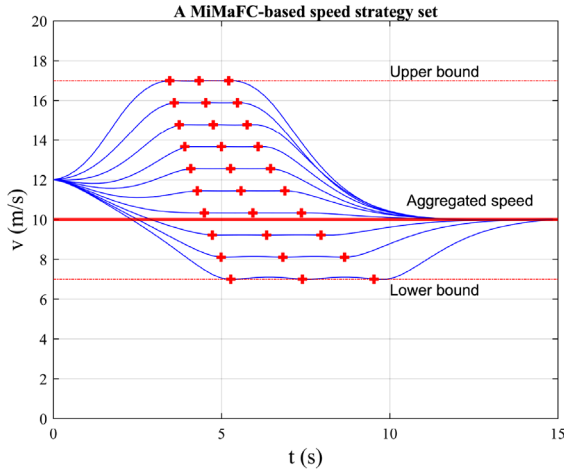
Our previous work has applied a collective intelligent optimisation algorithm to search feasible solutions with self-interested speed strategy set (see Figure 5(b)). More specifically, there are N_i self-interested options for each vehicle depending on the initial speed $v_i(0)$ (for instance $N_i = 10, v_i(0) = 12 \text{ m/s}$ in Figure 5(b)). By both considering the safety and comfort requests, intersection has a speed limit in the upper and lower bounds and vehicles tend to restrict acceleration a_i (e.g. $a_i \in [-2 \text{ m/s}^2, 2 \text{ m/s}^2]$) within certain time intervals $[0, T]$. A further taken hypothesis is that all the vehicles will get a fixed speed $v_i(T)$ after a predefined action time t_{act} (such as $t_{act} = 3 \text{ s}$ in Figure 5(b)). At last, a self-interested speed strategy set for vehicle can be summarised as a tuple $\{v_i(T), t_{act}, N_i\} (t \in [0, T])$. Readers interested in the creation of self-interested speed profiles are encouraged to consult earlier works [25]. However, the bounded conditions (e.g. the initial speed) are sensitive for CAVs system navigation in the proposed road network. In fact, self-interested velocity planning is preferable in order to request for vehicle cooperation in closing CA and ensuring 100% navigation safety. As a consequence, the strategy set of sampled speed profiles is refined in this study using a spatio-temporal velocity adaptation mechanism, with the MiMaFC info from the local supervisor’s policy.

Spatio-temporal velocity adaption:

As mentioned in previous section, a car will decelerate in S_1 until reaching P_0 (see Figure 4) to identify whether the considered vehicles will participate in the optimisation. See Figure 6(a), in the proposed spatio-temporal velocity adaption approach, the collaborative vehicle can firstly choose the actions at P_0 . If it cannot find any feasible solution at P_0 (or other DMP $P_i \in (P_0, P_f)$), the vehicle will go on decelerating phase regarding previous speed during one decision-making interval (e.g. 0.1 s). Importantly, the sorting algorithm (cf. Algorithm 1) will not identify the vehicle as a collaborative agent. During deceleration, a vehicle (and the car that follows it) must maintain a safe distance through the car-following model in Equation (3). Thus, the vehicle rerun the optimisation after arbitrary time steps at DMP P_i (belong to MiMaFC-DMA) and generate a set of possible speed profiles with lower initial speed. Generally, as seen in Figure 6(a), the speed profiles (blue line) have a constraint (red dotted line) of the acceptable range and final target speed (red line). The addressed aggregated speed \mathbb{V}_{L_i} in MiMaFC policy are defined as the reference speed v_{ref} for each direction. Additionally, the sampled speed must keep constants when entering CA (see Figure 4) to ease the system complexity associated with developing more practical vehicle crossing solutions. Thus, the sampled speed interval can be addressed regard-



(a) Displacement-velocity profiles in a local area



(b) A MiMaFC-based speed strategy set

FIGURE 6 A spatio-temporal velocity adaption approach for CAVs' developing speed strategy at the supervised intersection

ing different constant speeds in CA within the upper/lower bound.

4.2.2 | Numerical solutions for MiMaFC-based strategy

The generation of predefined speed profiles from the MiMaFC-based velocity set are inspired by refs. [51, 52]. Indeed, the speed profile set is calculated based on predictive time horizon, as defined by Model Predictive Control (MPC). Thus, a cost function f with initial state $\mathbf{x}_k = (v_k - v_{\text{ref}}, a_k)^T$ (recall that v_k, a_k is the ego vehicle speed/acceleration, v_{ref} is the reference speed for exiting) is created in this paper. Moreover, jerk (links which influence the physiological aspects of the passenger) is denoted as the input signal $\mathbf{u}_k \in [\mathbf{u}_{\min}, \mathbf{u}_{\max}]$ in f . Thus, the

running-cost (integral-cost) is modelled as follows:

$$f = \sum_{i=1}^{N_{\text{opt}}} \mathbf{x}_{k+i}^T \mathbf{Q} \mathbf{x}_{k+i} + \mathbf{u}_{k+i-1}^T \mathbf{R} \mathbf{u}_{k+i-1} \quad (11)$$

Where, \mathbf{Q} and \mathbf{R} are the positive-definite matrix weights to penalise the state error and system input respectively. N_{opt} is the maximum optimisation step number after the discretisation of the predicted horizon. Then, the dynamics model of the proposed system can be explicitly defined as follows:

$$\mathbf{x}_{k+1} = \mathbf{A} \mathbf{x}_k + \mathbf{B} \mathbf{u}_k \quad (12)$$

$$\mathbf{A} = \begin{bmatrix} 1 & \Delta t \\ 0 & 1 \end{bmatrix}, \mathbf{B} = \begin{bmatrix} 0 \\ \Delta t \end{bmatrix}, \mathbf{x}_k = \begin{bmatrix} v_k - v_{\text{ref}} \\ a_k \end{bmatrix}$$

Hence, it is possible to recast the quadratic optimisation problem into the whole prediction time horizon with any initial state \mathbf{x}_k by introducing the vectors $\bar{\mathbf{x}}_{k+1}$, $\bar{\mathbf{u}}_k$, $\bar{\mathbf{Q}}$, and $\bar{\mathbf{R}}$ in the form:

$$\bar{\mathbf{x}}_{k+1} = \begin{bmatrix} \mathbf{x}_{k+1} \\ \mathbf{x}_{k+2} \\ \vdots \\ \mathbf{x}_{k+N_{\text{opt}}} \end{bmatrix}, \bar{\mathbf{u}}_k = \begin{bmatrix} \mathbf{u}_k \\ \mathbf{u}_{k+1} \\ \vdots \\ \mathbf{u}_{k+N_{\text{opt}}-1} \end{bmatrix} \quad (13)$$

$$\bar{\mathbf{Q}} = \begin{bmatrix} \mathbf{Q} & & & \\ & \ddots & & \\ & & \mathbf{Q} & \\ & & & \mathbf{Q} \end{bmatrix}, \bar{\mathbf{R}} = \begin{bmatrix} \mathbf{R} & & & \\ & \ddots & & \\ & & \mathbf{R} & \\ & & & \mathbf{R} \end{bmatrix}$$

The running-cost function f in Equation (11) can be rewritten as:

$$f = \bar{\mathbf{x}}_{k+1}^T \bar{\mathbf{Q}} \bar{\mathbf{x}}_{k+1} + \bar{\mathbf{u}}_k^T \bar{\mathbf{R}} \bar{\mathbf{u}}_k \quad (14)$$

Further, the state space model in Equation (12) is correspondingly formulated as:

$$\bar{\mathbf{x}}_{k+1} = \bar{\mathbf{A}} \mathbf{x}_k + \bar{\mathbf{B}} \bar{\mathbf{u}}_k \quad (15)$$

$$\bar{\mathbf{A}} = \begin{bmatrix} \mathbf{A} \\ \mathbf{A}^2 \\ \vdots \\ \mathbf{A}^{N_{\text{opt}}} \end{bmatrix}, \bar{\mathbf{B}} = \begin{bmatrix} \mathbf{B} & 0 & \cdots & 0 \\ \mathbf{A}\mathbf{B} & \mathbf{B} & \cdots & 0 \\ \vdots & \vdots & \ddots & \vdots \\ \mathbf{A}^{N_{\text{opt}}}\mathbf{B} & \mathbf{A}^{N_{\text{opt}}-1}\mathbf{B} & \cdots & \mathbf{B} \end{bmatrix}$$

Finally, we substitute Equation (15) into Equation (14) to reserve only the input matrix $\bar{\mathbf{u}}$ by a standard quadratic form:

$$f(\bar{\mathbf{u}}_k) = \frac{1}{2} \bar{\mathbf{u}}_k^T \mathbf{H} \bar{\mathbf{u}}_k + \mathbf{f} \bar{\mathbf{u}}_k + \mathbf{d}_k \quad (16)$$

$$\mathbf{H} = 2(\bar{\mathbf{B}}^T \bar{\mathbf{Q}} \bar{\mathbf{B}} + \bar{\mathbf{R}}_k)$$

$$\mathbf{f} = 2(\bar{\mathbf{A}} \mathbf{x}_k)^T \bar{\mathbf{Q}} \bar{\mathbf{B}}$$

$$\mathbf{d}_k = (\bar{\mathbf{A}} \mathbf{x}_k)^T \bar{\mathbf{Q}} \bar{\mathbf{A}} \mathbf{x}_k$$

TABLE 1 Parameters adopted in the tackled scenario

Module	Parameters	Notation	Value	Units
Traffic background	Simulation time	T_{end}	60–120	s
	Sampled time interval	T_{sample}	0.2	s
	Sampled point interval	T_{pts}	0.2	m
	The radius of $\mathcal{J}_{\text{Loc},i}$	R	65	m
	Vehicle safe radius	r	3	m
	Lane length	L	410	m
	Lane speed limit	$[v_{\text{min}}, v_{\text{max}}]$	[0.2, 20]	m/s
	Bounds on acceleration	$[a_{\text{min}}, a_{\text{max}}]$	[-3, 3]	m/s ²
	Bounds on jerk	$[j_{\text{min}}, j_{\text{max}}]$	[-2, 2]	m/s ³
	Initial speed for all the vehicle	v_{initial}	$8 \pm 2/10 \pm 2$	m/s
Local supervisor	Minimum 2D time-to-collision	TTC_{min}	10	s
	Reference acceleration in ACC mode	a_{ref}	1.5	m/s ²
	Local area division	$\{\mathcal{J}_1, \mathcal{J}_2, \mathcal{J}_3\}$	{20, 15, 35}	m
	Target speed for vehicle leave in CC mode (equal to v_{max})	v_{end}	20	m/s
Car-following model	CC reference acceleration to maximum speed v_{max}	a_{ref}	1.5	m/s ²
	ACC Control gains	$\{k_0, k_1, k_2\}$	{1, 1, 3}	-
	Log-normal distribution parameters	$\{\mu_p, \sigma_p\}$	{0.73, 0.52}	-
	Standstill safe distance	d_{safe}	6	m
	Sensing range	R_w	30	m
Optimisation model	Strategy number	N_s	10	-
	Matrix weight for strategy	$\{Q, R\}$	$\begin{Bmatrix} 1 & 0 \\ 0 & 1 \end{Bmatrix}, \begin{Bmatrix} 0 & 0 \\ 0 & 1 \end{Bmatrix}$	-
	Prediction horizon	T_{horizon}	15	s
	Weight on exit speed	W_{speed}	0.5	-
	Weight on separation	W_{sep}	10	-
	Weight on crossing time	W_{cross}	0.5	-
	Max stable number	N_{stable}	4	-
	Final simulated temperature	Temp_{end}	0	-
	Max number of iterations	$N_{\text{iteration}}$	100	-
	Initial simulated temperature	Temp_{ini}	10	-

Where the quadratic part described by \mathbf{H} and linear part described by \mathbf{f} will influence the input $\bar{\mathbf{u}}_k$. Therefore, the independent part \mathbf{d}_k (constant related to the initial state \mathbf{x}_k) in Equation (16) can be eliminated to make the objective function f running more compactly. Thus, the proposed quadratic optimisation problem can be defined as:

$$\begin{aligned} \min_{\bar{\mathbf{u}}_k} \quad & f^*(\bar{\mathbf{u}}_k) = \frac{1}{2} \bar{\mathbf{u}}_k^T \mathbf{H} \bar{\mathbf{u}}_k + \mathbf{f} \bar{\mathbf{u}}_k \\ \text{subject to} \quad & A_{\text{ineq}} \bar{\mathbf{u}}_k \leq b_{\text{ineq}} \\ & A_{\text{eq}} \bar{\mathbf{u}}_k = b_{\text{eq}} \end{aligned} \quad (17)$$

Where $\bar{\mathbf{u}}_k$ belongs to the bounds of $[\bar{\mathbf{u}}_{\text{lower}}, \bar{\mathbf{u}}_{\text{upper}}]$ regarding the inequality constrains. The equality constrains are used to enforce the speed to keep constant at CA (see Figure 4). If a car enters the conflict area at i_1 and exit at i_2 where $i_1, i_2 \in$

$\{1, \dots, N_{\text{opt}}\}$, the constraints can be addressed as:

$$\begin{aligned} A_{\text{ineq}} &= \begin{bmatrix} \mathbf{I} \\ -\mathbf{I} \end{bmatrix}, b_{\text{ineq}} = \begin{bmatrix} \bar{\mathbf{u}}_{\text{upper}} \\ -\bar{\mathbf{u}}_{\text{lower}} \end{bmatrix} \\ A_{\text{eq}} &= \begin{bmatrix} [\overline{CB}]_{i_1,*} \\ [\overline{CB}]_{i_2,*} \end{bmatrix}, b_{\text{eq}} = \begin{bmatrix} [-CA\mathbf{x}_k]_{i_1,*} + \bar{v}_{\text{ref}} \\ [-CA\mathbf{x}_k]_{i_2,*} + \bar{v}_{\text{ref}} \end{bmatrix} \end{aligned} \quad (18)$$

Where:

$$\bar{C} = \begin{bmatrix} C & & \\ & \ddots & \\ & & C \end{bmatrix}, C = [1, 0] \quad (19)$$

$$\bar{v}_{\text{ref}} = v_s - v_{\text{ref}}$$

$$v_{\text{ref}} = \min\{V_L, v_{\text{upper}}\}, \quad V_L \in [V_{L_1}, V_{L_2}, V_{L_3}, V_{L_4}]$$

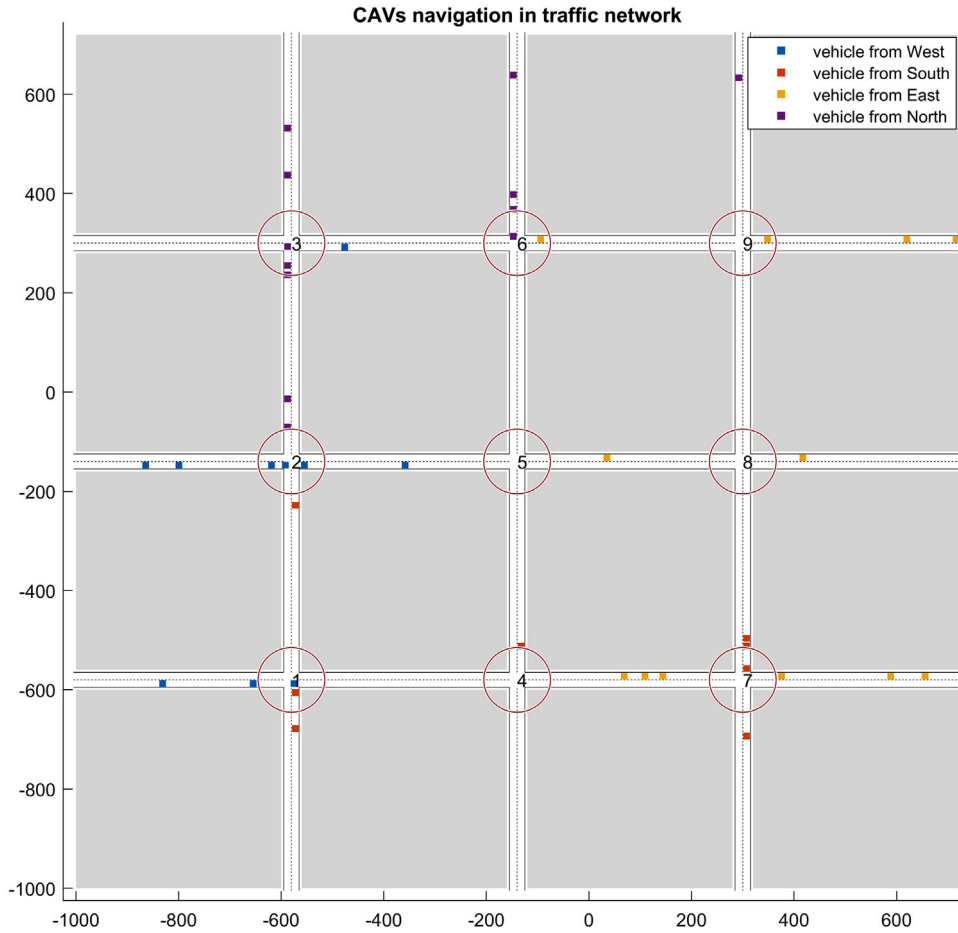


FIGURE 7 Unidirectional flow of CAVs navigation in traffic network for both supervised and unsupervised system. The red circles stand for the covered range of a local supervisor $S_{L,CA}$ noted from 1 to 9. (simulation videos can be found at <https://bit.ly/3zcDwAu>)

In Equation (18), $[\overline{CB}]_{i,*}$ and $[-\overline{CA}\mathbf{x}_k]_{i,*}$ stand for the row i in matrix \overline{CB} and $-\overline{CA}\mathbf{x}_k$. The sampled speed v_s (between the bounds of $[v_{lower}, v_{upper}]$) are defined as the constant speed in CA. The reference speed v_{ref} is defined according to the aggregated speed \mathbb{V}_L in the targeted direction or local speed limit. More precisely, the final speed of the vehicle either tends toward the maximum allowed speed v_{upper} in the intersection or reach the traffic aggregated speed (if $\mathbb{V}_L < v_{upper}$). Therefore, the numerical solutions (i.e. the possible MiMaFC-based speed strategy set) for the quadratic programming are given by various sampled v_s . As seen in Figure 6(b), the red plus signs present the time vehicle entering the conflict area by ten sampled speeds $v_s \in [7, 17]$ m/s. All proposed speed profiles are converged to the lane aggregated speed $\mathbb{V}_L = 10$ m/s (red line) at the end of the time horizon.

5 | SIMULATIONS

To illustrate the performance of the proposed methods in this paper, the next generation simulation (NGSIM) data sets are explored to characterise the stochastic time headway distribu-

tion (i.e. $\hat{t}h_i \sim \log-N$) for macroscopic flow model. Further, simulations are developed in MATLAB SimEvents to evaluate the proposed traffic management system MHCP-MP. The main parameters adopted in the tackled scenario are summarised in Table 1.

5.1 | Instances

The verified scenario can be seen in Figure 7. The overall MHCP-MP framework was run in 3×3 urban road networks. The unidirectional flows arrive from outside of the network according to a Poisson distribution with the default parameter $\lambda = 1.5$ veh/s. Road segments are 410 m long. Each intersection's width is 30 m. A local supervisor located in the centre of each intersection and authorised for a 65 m radius (see Figure 7). Outside the intersection area, an adaptive cruise control (ACC) system is adopted for maintaining a desired reference speed $v_{ref} = 20$ m/s or time headway linking the log-normal distribution (see $\{\mu_v, \sigma_v\}$ in Table 1). The safe radius of each vehicle is 3 m. Consequently, the minimum safe distance between any two vehicles is 6 m.

TABLE 2 A comparison of intersection management for urban traffic flow

Model	Instance	Run time	Initial speed (m/s)	Vehicles' number	Conflicted frequency	Switch frequency	Average crossing time (s)
Spatio-temporal velocity adaption	Trial 1	60 s	8 ± 2	42	0	0	9.6467
	Trial 2	60 s	10 ± 2	42	0	0	9.6867
	Trial 3	90 s	8 ± 2	71	0	4	10.6590
	Trial 4	90 s	10 ± 2	71	0	4	10.5846
	Trial 5	120 s	8 ± 2	93	12	22	11.3566
	Trial 6	120 s	10 ± 2	93	9	20	11.3057
MiMaFC-based strategy	Trial 1	60 s	8 ± 2	42	0	-	9.6467
	Trial 2	60 s	10 ± 2	42	0	-	9.6867
	Trial 3	90 s	8 ± 2	71	0	-	10.6949
	Trial 4	90 s	10 ± 2	71	0	-	10.7744
	Trial 5	120 s	8 ± 2	93	16	-	11.4799
	Trial 6	120 s	10 ± 2	93	13	-	11.4656
Self-interested strategy	Trial 1	60 s	8 ± 2	42	2	-	6.4571
	Trial 2	60 s	10 ± 2	42	0	-	6.4545
	Trial 3	90 s	8 ± 2	71	10	-	6.4578
	Trial 4	90 s	10 ± 2	71	11	-	6.4536
	Trial 5	120 s	8 ± 2	93	19	-	6.4583
	Trial 6	120 s	10 ± 2	93	22	-	6.4616
First-come first-served (FCFS) strategy	Trial 1	60 s	8 ± 2	42	1	-	13.3333
	Trial 2	60 s	10 ± 2	42	0	-	13.5692
	Trial 3	90 s	8 ± 2	71	13	-	13.3711
	Trial 4	90 s	10 ± 2	71	7	-	13.4179
	Trial 5	120 s	8 ± 2	93	49	-	13.4605
	Trial 6	120 s	10 ± 2	93	39	-	13.4203

5.2 | Comparative approaches

For each instance, we compare our method with three different intersection network control techniques.

- Spatio-temporal velocity adaptation approach: it follows a division of intersection areas to calculate a position-dependent velocity strategy while taking global performance into account (cf. subsection 4.1.3). A local supervisor S_{Loc_A} is anticipated to be deployed at each intersection to manage all cars in accordance with the specified navigation protocols.
- MiMaFC-based strategy [40]: it was initially proposed in our previous work and improved with more precise numeration solutions in this work (cf. subsection 4.2.2). It was designed primarily to increase traffic efficiency. In addition, a local supervisor S_{Loc_A} is necessary for this strategy. It is used to evaluate the capability of optimising vehicle trajectories without dividing the intersection area.
- Self-interested strategy [25]: it was developed for a negotiation-based system that requires no further local supervision. All cars near the intersection must negotiate a crossing trajectory corresponding with the established self-interested

strategy (cf. subsection 4.2.1). Global traffic performance was omitted. It is used to evaluate the performance of the entire unsupervised decentralised CAVs systems.

- First-come-first-served (FCFS) strategy (motivated by ref. [33]): it works on a reservation-based system. Intuitively, vehicles arriving first are given priority service and are permitted entry into an intersection. The algorithm is widely used in the AIM-based reservation strategies [33]. According to current studies [53], AIM is more effective than traffic lights (periodic signalling) for unsignalised intersection control. Thus, we evaluate the performance of the proposed techniques (trajectory-based) with a reservation-based system using the FCFS mechanism.

5.3 | Goals

We have conducted numerical experiments to collect data regarding the following issues:

- Decision-making (microscopic): the capacity of each method to provide feasible and effective solutions, as well as their

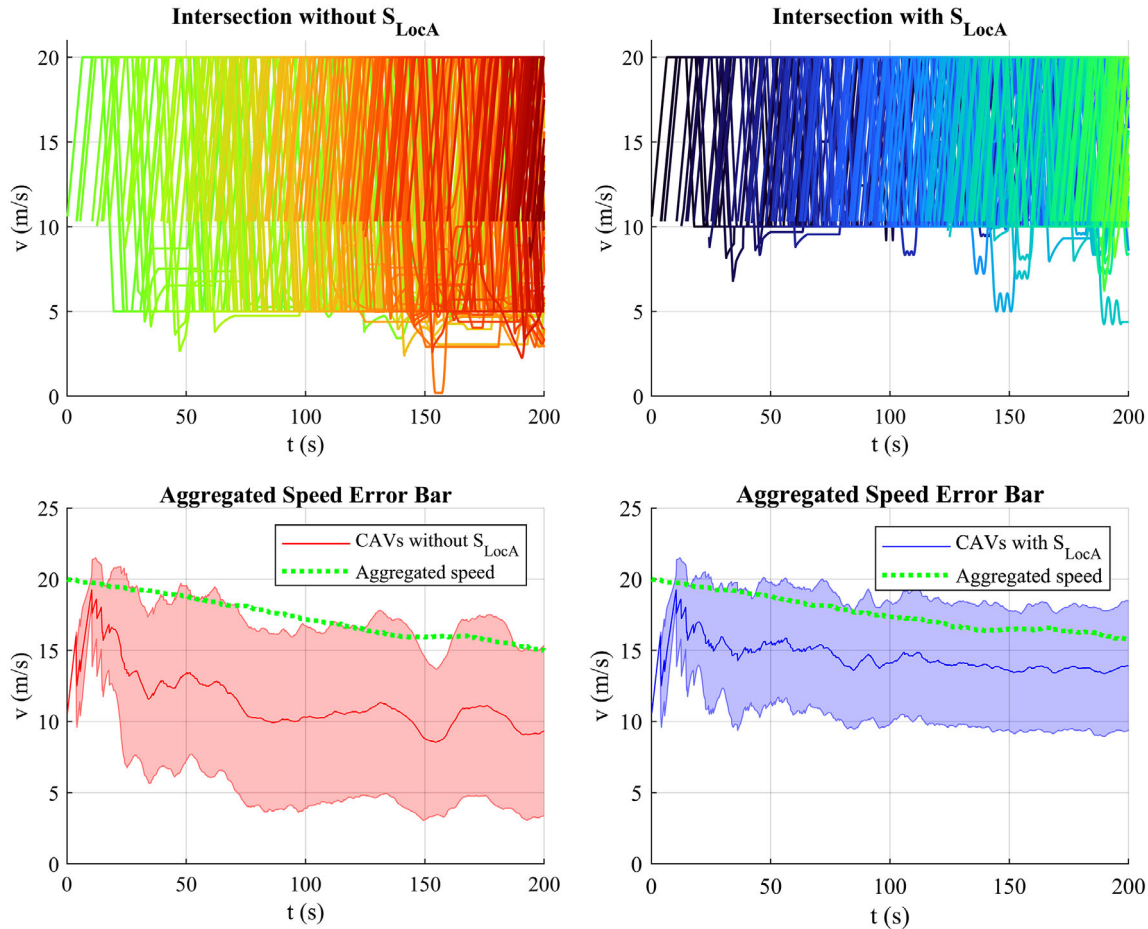


FIGURE 8 A Comparison of CAVs velocities between MHCP-MP framework with S_{LocA} and baseline method without S_{LocA} . An augmented navigation protocol was also implemented in the MHCP-MP framework

dependency on simulation duration, vehicle number, and random initial speed. For the spatio-temporal velocity adaptation method, we additionally consider the frequency of switching between the two predefined intersection strategies.

- Local supervisor (management): the sensitivity of our algorithm to the MiMaFC policy from the local supervisor S_{LocA} . The cooperative navigation performance of CAVs is tested primarily in terms of traffic flow and average speed using predefined traffic measurements.
- Traffic efficiency (macroscopic): verify better traffic efficiency using measurable traffic data from our macroscopic flow model.

The obtained results can be seen in the following:

As seen in Table 2, the performances of four intersection management techniques were shown with their individual trials and initial conditions that were generated randomly. The predetermined simulation times for each approach are 60, 90, and 120 s. In each trial, all of the vehicles were set up with an initial speed that varied randomly between 8 ± 2 m/s or 10 ± 2 m/s. The velocity bounds are specifically [0 m/s, 20 m/s] (as given in Table 1). In particular, the conflicted frequency represents the cumulative failure numbers that violated the

safe threshold. A high conflicted frequency (for each trial) demands re-planning, which also incurs additional computational costs. All intersection management strategies will have a high frequency of inefficient solution as the number of vehicles increases (equal to an increased traffic flow). Particularly with a lesser traffic flow (e.g. vehicle number equal to 42), all strategies might maintain a low conflicted frequency (for each trial). Specifically, spatio-temporal velocity adaptation strategy and MiMaFC-based strategies may ensure successful decision-making all the way during the simulation time in trial 1~6. With a large volume of traffic (93 vehicles), the MiMaFC-based approach performs better than the self-interested strategy in both trials 5 and 6. Remarkably, the approach of spatio-temporal velocity adaptation might greatly reduce the conflicted frequency. It demonstrates that the technique suggested in this work may better manage a large traffic volume and hence produce more effective responses to traffic uncertainty. In addition, we see that the frequency of strategy switches in spatio-temporal velocity adaptation increases rapidly with simulation time (e.g. from 0 to 22). It reveals that the technique of switch strategy is recommended for vehicle cooperation in different areas that are divided by a local supervisor S_{LocA} . In addition, it seems that the different initial speeds have an effect on all

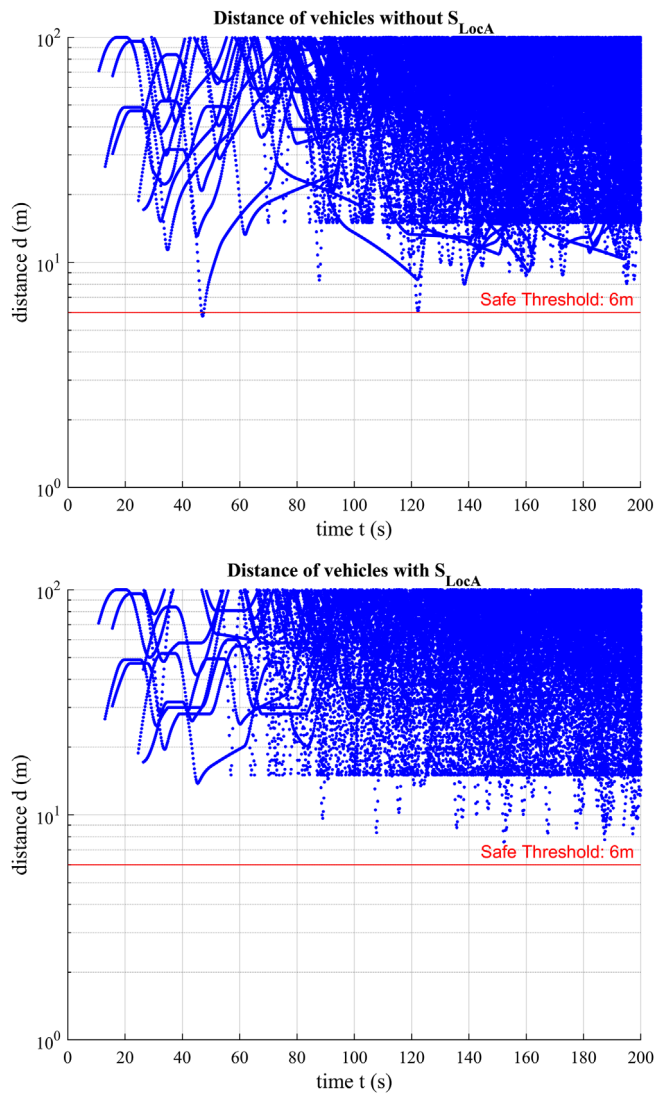


FIGURE 9 A comparison of inter-vehicle distance in traffic network

the methods. Moreover, only CA in an interaction are managed by a reservation-based system under the FCFS strategy. Consequently, the FCFS method results in multiple conflicts, particularly in the long run at road upstream. Due to the need for vehicles to decelerate while waiting for the order to pass, FCFS results in the longest average crossing time for each intersection area. In a fully decentralised system, the self-interested method performs best in terms of the average crossing time. In general, the four intersection management strategies perform similarly with low vehicle numbers. However, the suggested spatio-temporal velocity adaptation approach in this paper may perform better in assisting CAVs in finding feasible solutions throughout the decision-making process as traffic volume increases.

Next, experiments were performed in a simulation of 200 s to validate the local supervisor's capacity to suggest MiMaFC policy. More precisely, the self-interested strategy (without S_{Loc_A}) and the proposed method spatio-temporal velocity adaptation

approach (with S_{Loc_A}) were evaluated under identical initial circumstances (initial speed 10 m/s and number of vehicles).

As seen in Figure 8, the up-left and up-right velocity diagram give a global view of baseline model (self-interested strategy) without S_{Loc_A} and the proposed method with S_{Loc_A} (spatio-temporal velocity adaptation approach). The desired exit speed in the baseline model is equal to the maximum speed in their strategy set. Although vehicles expect to leave the intersection as fast as possible, CAVs have to wait for their turn to participate in the decision-making. In such an approach, the maximum allowed agents can participate the optimisation is five. Therefore, the remained CAVs in the local area have to slow down until permit to participate in cooperative optimisation. Moreover, the initial speed is very sensitive to vehicle's decision-making (as indicated in Table 2). A decelerate policy was widely adopted before entering the intersection in the unsupervised CAVs system. Simulations show that vehicle decelerates to around 5 m/s in order to have the ability to find the maximum admissible crossing strategy in predefined conditions. Nevertheless, due to the speed fluctuation, the desired velocity causally collapsed to 0 m/s when the vehicles increase during the second half simulation time. In contrast, CAVs adopting the I2V technology can obtain the real time traffic policy by S_{Loc_A} . The vehicle exit speed was expected to be close to the aggregated speed, which can help to harmonise the flow fluctuation. The augmented navigation protocol also wins the chance to find optimal (or sub-optimal) crossing strategy at relative high speed. The up-right velocity diagram in Figure 8 shows most vehicles can deal with the cooperative navigation task when a self speed greater than 10 m/s.

As a consequence, the proposed MHCP-MP framework including S_{Loc_A} can improve the average velocity (blue line in bottom-right graph in Figure 8) comparing with the whole distribute CAVs system's average speed (red line in bottom-left graph in Figure 8). In addition, all the adjacent vehicles keep a safe distance $d_{safe} = 6$ m in the addressed approach. On the contrary, twice violations of inter-vehicle distance are observed in the baseline model as seen in Figure 9. In brief, the overall cooperative CAVs system can benefit from the augmented navigation protocol and assigned real-time traffic policy of S_{Loc_A} to guarantee reliable, smooth, and safe running.

Finally, we utilise the measured traffic statistics to ensure the performance of the supervised system. The corresponding traffic fundamental diagram for each intersection and the exits of the whole urban network can be seen in Figure 10. The colour bar stands for the time in the depicted flow-density diagram. One can find that the vehicle density in the unsupervised CAVs system was unevenly distributed at various intersections. The flow decreases with the system running (e.g. intersection 1). Correspondingly, the output flow of the intersection network was showed at the bottom-left of Figure 10. The approximate maximum output flow is 300 Vehs/h. After that, it dropped to a lower value. Nevertheless, the proposed method maintains a promising traffic flow-density performance within the same input flow rate. The S_{Loc_A} can regulate the traffic flow by considering the "road weights" linking to the road density.

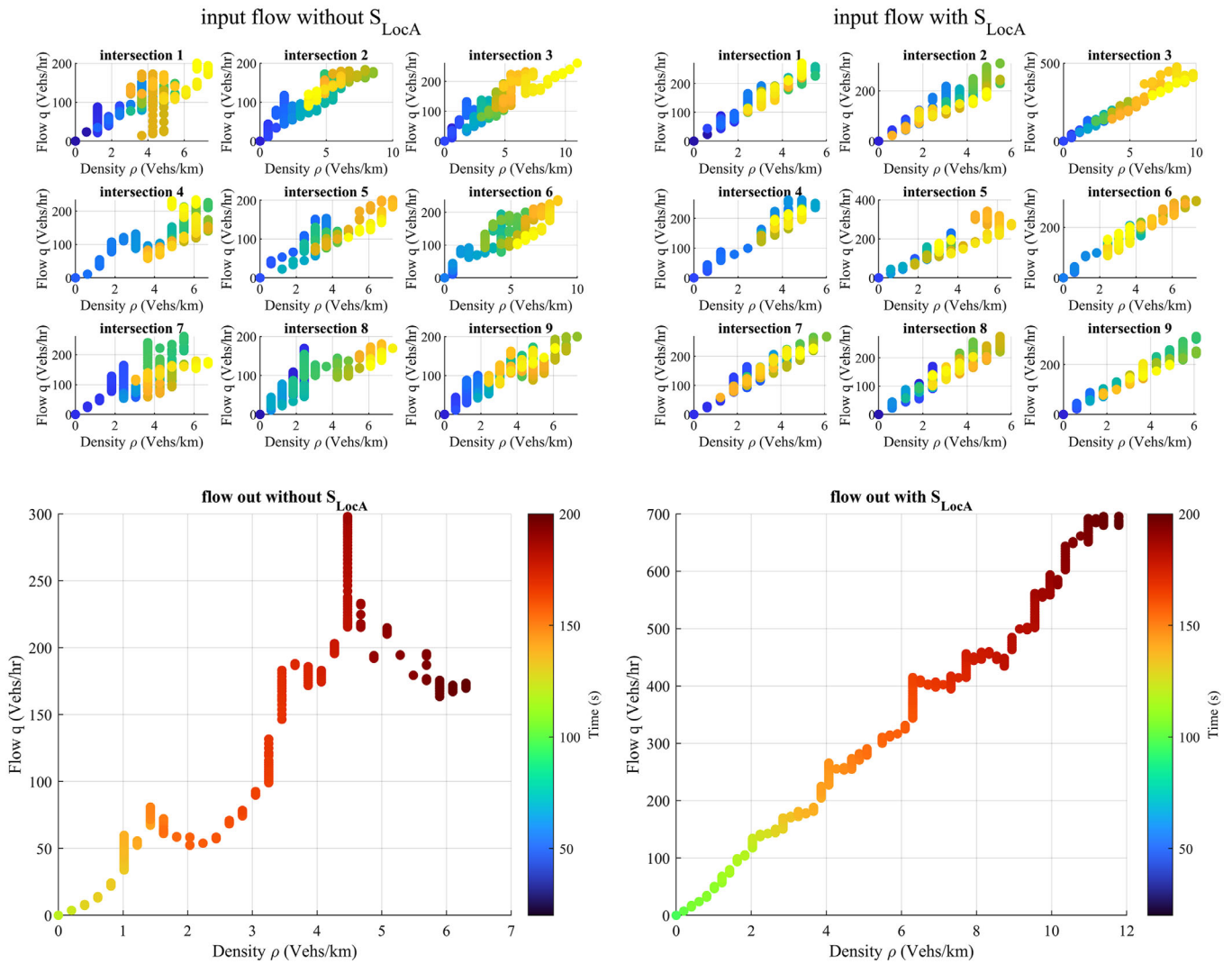


FIGURE 10 Traffic flow-density diagrams for intersections and output flow in whole exits

Therefore, a proportional increase in the flow-density diagram has been observed during the whole simulation time. Additionally, the output flow with S_{LocA} remarkably increase to 700 Vehs/h at the end (see the bottom-right graph of Figure 10). Similarly, the traffic oscillation of the CAVs system can be explained by Figure 11. More precisely, one of the most critical aspects of increasing traffic efficiency is dealing with traffic oscillations. Traffic oscillation is a term that refers to the stop-and-go driving situations that occur in heavy traffic and often result in bottlenecks in transportation networks. As seen in Figure 11, the displacement-time graphs were exhibited in up-left (unsupervised system) and up-right (supervised system) graph. A shock wave (congestion state) was induced between vehicles in the same lane when the ahead agents change their speeds. In contrast, the traffic congestion was alleviated in the supervised system which can adjust the traffic state properly. In addition, single vehicle displacement can be improved by the proposed system with S_{LocA} . See bottom graph of Figure 11, the colour bar represents the displace for each vehicle. Roughly,

vehicles in the supervised system shows a better mobility in the transportation system.

6 | CONCLUSION

In this paper, we explored the MHCP-MP architecture for CAVs' cooperative navigation in a road network based on the prior works [39, 40]. First, an overview of the planned MHCP-MP traffic scenario is given. We then built a macroscopic flow model to determine proposed CAVs navigation references (speeds, passing rights) based on traffic flow fluctuation. Thus, the high-hierarchical MiMaFC-based policy can ensure that the reference behaviour in micro motion control is applied robustly in response to traffic flow changes. Based on the developed MHCP-MP architecture, this study offered a cooperative navigation protocol to efficiently decide each agent's motion planning approach. In a highly networked environment, the procedure was done by a local supervisor. Furthermore, the

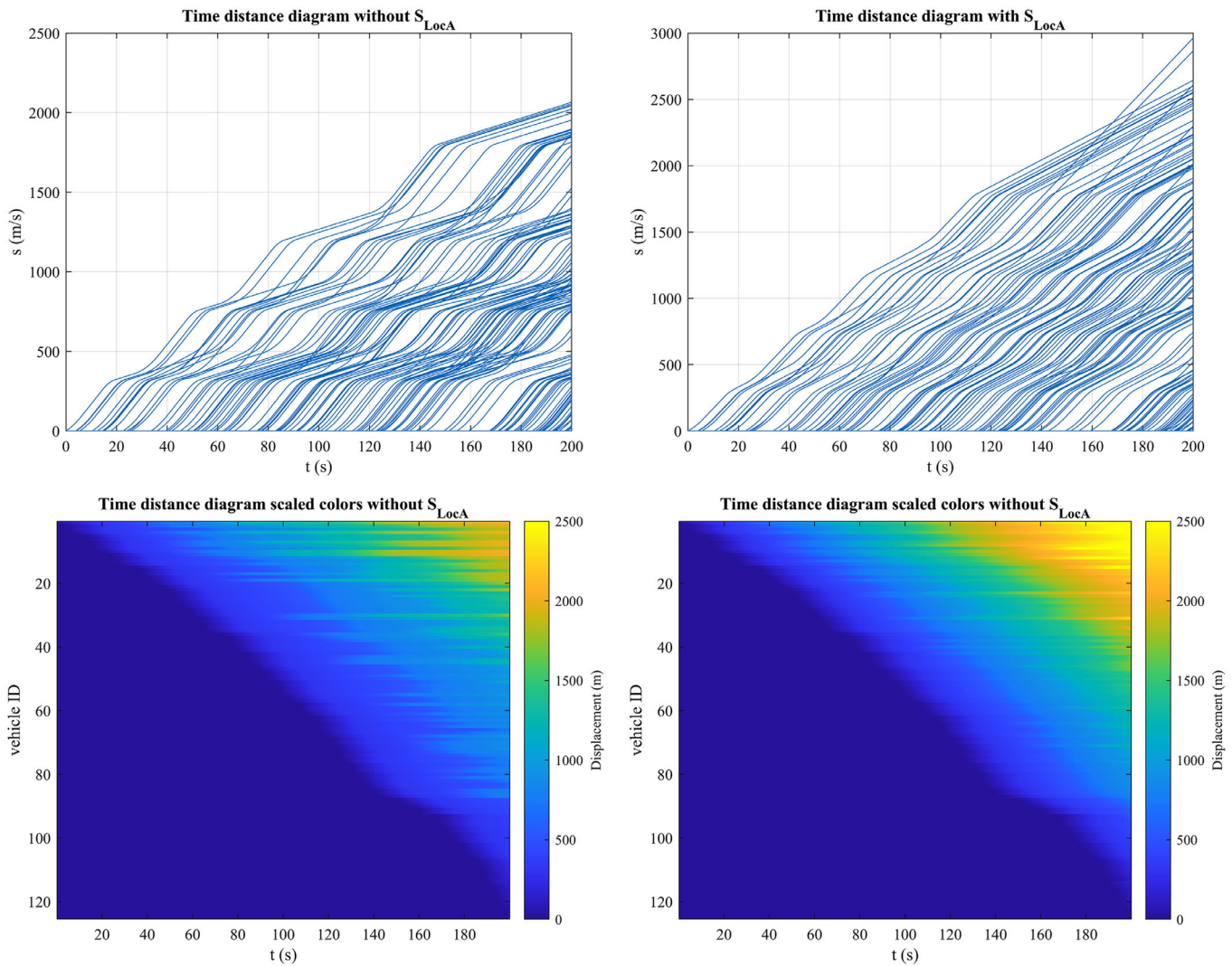


FIGURE 11 The traffic displacement diagram for the whole vehicles

spatio-temporal velocity adaption technique proposed in this paper also improves the microscopic CAVs optimisation model for AIM. The local conflict resolution strategy can be easily calculated by adopting the velocity adaption approach. Quadratic programming is employed in particular to provide the numerical solution for the proposed MiMaFC-based velocity strategy set. Simulation results indicate an overall improvement in traffic flow control. At an unsignalised intersection, the local supervisor S_{LocA} can guide the CAVs' motion planning, so enhancing cooperative navigation efficiency.

This study's future work can be extended in different directions. For instance, it is critical to investigate the proposed traffic management/vehicle control architecture's ability to handle heterogeneous traffic flows. Moreover, the future research should include real-world testing or large-scale simulation based on real-world traffic data.

ACKNOWLEDGMENTS

This work has been sponsored by the Chinese Ministry of Industry and Information Technology (MIIT) research

program "the 2020 Innovative Development of the Industrial Internet" (TC200H033 and TC200H01F), by the Dongfeng Motor Corporation "Project 928" (DF928-2020-040). This work received also the support by the French government research program "Investissements d'Avenir" through the IMoBS3 Laboratory of Excellence (ANR-10-LABX-16-01) and the CPER RITMEA, Hauts-de-France region.

CONFLICT OF INTEREST

The authors declare no conflict of interest.

AUTHOR CONTRIBUTIONS

zhengze ZHU: Writing - original draft. Lounis ADOUANE: Supervision, writing - review and editing. Alain QUILLIOT: Supervision.

DATA AVAILABILITY STATEMENT

The data that support the findings of this study are available from the corresponding author upon reasonable request.

ORCID

Zhengze Zhu  <https://orcid.org/0000-0002-9240-113X>

REFERENCES

- Guanetti, J., Kim, Y., Borrelli, F.: Control of connected and automated vehicles: state of the art and future challenges. *Annu. Rev. Control* 45, 18–40 (2018)
- Elliott, D., Keen, W., Miao, L.: Recent advances in connected and automated vehicles. *J. Traffic Transp. Eng. (Engl. Ed.)* 6(2), 109–131 (2019)
- Eskandarian, A., Wu, C., Sun, C.: Research advances and challenges of autonomous and connected ground vehicles. *IEEE Trans. Intell. Transp. Syst.* (2019)
- Sjoberg, K., Andres, P., Buburuzan, T., Brakemeier, A.: Cooperative intelligent transport systems in europe: current deployment status and outlook. *IEEE Veh. Technol. Mag.* 12(2), 89–97 (2017)
- Wang, Z., Bian, Y., Shladover, S.E., Wu, G., Li, S.E., Barth, M.J.: A survey on cooperative longitudinal motion control of multiple connected and automated vehicles. *IEEE Intell. Transp. Syst. Mag.* 12(1), 4–24 (2019)
- Papadoulis, A., Quddus, M., Imprialou, M.: Evaluating the safety impact of connected and autonomous vehicles on motorways. *Accid. Anal. Prev.* 124, 12–22 (2019)
- Pocztar, S.L., Jankovic, L.M., et al.: The Google Car: driving toward a better future? *J. Bus. Case Stud.* 10(1), 7–14 (2014)
- Fagnant, D.J., Kockelman, K.: Preparing a nation for autonomous vehicles: opportunities, barriers and policy recommendations. *Transp. Res. Part A: Policy Pract.* 77, 167–181 (2015)
- Vilca, J.M., Adouane, L., Mezouar, Y.: Reactive navigation of mobile robot using elliptic trajectories and effective on-line obstacle detection. *Gyroc. Navig. J.* 4(1), 14–25 (2013)
- Zhang, Y.J., Malikopoulos, A.A., Cassandras, C.G.: Optimal control and coordination of connected and automated vehicles at urban traffic intersections. In: 2016 American Control Conference (ACC), pp. 6227–6232. IEEE, Piscataway, NJ (2016)
- Rios-Torres, J., Malikopoulos, A.A.: A survey on the coordination of connected and automated vehicles at intersections and merging at highway on-ramps. *IEEE Trans. Intell. Transp. Syst.* 18(5), 1066–1077 (2016)
- Chen, N., Wang, M., Alkim, T., van Arem, B.: A robust longitudinal control strategy of platoons under model uncertainties and time delays. *J. Adv. Transp.* 2018, 9852721 (2018)
- Malikopoulos, A.A., Beaver, L., Chremos, I.V.: Optimal time trajectory and coordination for connected and automated vehicles. *Automatica* 125, 109469 (2021)
- Chen, D., Ahn, S., Chitturi, M., Noyce, D.A.: Towards vehicle automation: roadway capacity formulation for traffic mixed with regular and automated vehicles. *Transp. Res. Part B: Methodol.* 100, 196–221 (2017)
- Ghiasi, A., Li, X., Ma, J.: A mixed traffic speed harmonization model with connected autonomous vehicles. *Transp. Res. Part C: Emerg. Technol.* 104, 210–233 (2019)
- Pourmehr, M., Eleftheriadou, L., Ranka, S., Martin Gasulla, M.: Optimizing signalized intersections performance under conventional and automated vehicles traffic. *IEEE Trans. Intell. Transp. Syst.* 21(7), 2864–2873 (2019)
- Zhou, M., Yu, Y., Qu, X.: Development of an efficient driving strategy for connected and automated vehicles at signalized intersections: a reinforcement learning approach. *IEEE Trans. Intell. Transp. Syst.* 21(1), 433–443 (2019)
- Chen, L., Englund, C.: Cooperative intersection management: a survey. *IEEE Trans. Intell. Transp. Syst.* 17(2), 570–586 (2015)
- Rios Torres, J., Malikopoulos, A.A.: A survey on the coordination of connected and automated vehicles at intersections and merging at highway on-ramps. *IEEE Trans. Intell. Transp. Syst.* 18(5), 1066–1077 (2016)
- Namazi, E., Li, J., Lu, C.: Intelligent intersection management systems considering autonomous vehicles: a systematic literature review. *IEEE Access* 7, 91946–91965 (2019)
- Guo, Q., Li, L., Ban, X.J.: Urban traffic signal control with connected and automated vehicles: a survey. *Transp. Res. Part C: Emerg. Technol.* 101, 313–334 (2019)
- Li, L., Wen, D., Yao, D.: A survey of traffic control with vehicular communications. *IEEE Trans. Intell. Transp. Syst.* 15(1), 425–432 (2013)
- Xu, Y., Zhou, H., Ma, T., Zhao, J., Qian, B., Shen, S.: Leveraging multi-agent learning for automated vehicles scheduling at non-signalized intersections. *IEEE Internet Things J.* 8(14), 11427–11439 (2021)
- Chen, X., Xu, B., Qin, X., Bian, Y., Hu, M., Sun, N.: Non-signalized intersection network management with connected and automated vehicles. *IEEE Access* 8, 122065–122077 (2020)
- Philippe, C., Adouane, L., Tsourdos, A., Shin, H.S., Thuilot, B.: Probability collectives algorithm applied to decentralized intersection coordination for connected autonomous vehicles. 2019 IEEE Intelligent Vehicles Symposium (IV), pp. 1928–1934. IEEE, Piscataway, NJ (2019)
- Zhu, Z., Adouane, L., Quilliot, A.: A decentralized multi-criteria optimization algorithm for multi-unmanned ground vehicles (MUGVS) navigation at signal-free intersection. *IFAC-PapersOnLine* 54(2), 327–334 (2021)
- Zhu, Z., Adouane, L., Quilliot, A.: Flexible multi-unmanned ground vehicles (mugvs) in intersection coordination based on ϵ -constraint probability collectives algorithm. *Int. J. Intell. Rob. Appl.* 5(2), 156–175 (2021)
- Katrakazas, C., Quddus, M., Chen, W.H., Deka, L.: Real-time motion planning methods for autonomous on-road driving: state-of-the-art and future research directions. *Transp. Res. Part C: Emerg. Technol.* 60, 416–442 (2015)
- Florin, R., Olariu, S.: A survey of vehicular communications for traffic signal optimization. *Veh. Commun.* 2(2), 70–79 (2015)
- Olia, A., Abdelgawad, H., Abdulhai, B., Razavi, S.N.: Assessing the potential impacts of connected vehicles: mobility, environmental, and safety perspectives. *J. Intell. Transp. Syst.* 20(3), 229–243 (2016)
- Baskar, L.D., De Schutter, B., Hellendoorn, J., Papp, Z.: Traffic control and intelligent vehicle highway systems: a survey. *IET Intell. Transp. Syst.* 5(1), 38–52 (2011)
- Wang, Z., Wu, G., Barth, M.J.: Cooperative eco-driving at signalized intersections in a partially connected and automated vehicle environment. *IEEE Trans. Intell. Transp. Syst.* 21(5), 2029–2038 (2019)
- Hausknecht, M., Au, T.C., Stone, P.: Autonomous intersection management: multi-intersection optimization. In: 2011 IEEE/RSJ International Conference on Intelligent Robots and Systems, pp. 4581–4586. IEEE, Piscataway, NJ (2011)
- Levin, M.W., Fritz, H., Boyles, S.D.: On optimizing reservation-based intersection controls. *IEEE Trans. Intell. Transp. Syst.* 18(3), 505–515 (2016)
- Wuthishuwong, C., Traechtler, A.: Coordination of multiple autonomous intersections by using local neighborhood information. In: 2013 International Conference on Connected Vehicles and Expo (ICCVE), pp. 48–53. IEEE, Piscataway, NJ (2013)
- Schepperle, H., Böhm, K.: Auction-based traffic management: towards effective concurrent utilization of road intersections. In: 2008 10th IEEE Conference on E-Commerce Technology and the Fifth IEEE Conference on Enterprise Computing, E-Commerce and E-Services, pp. 105–112. IEEE, Piscataway, NJ (2008)
- Riener, A., Ferscha, A.: Enhancing future mass ICT with social capabilities. In: Co-evolution of Intelligent Socio-technical Systems, pp. 141–184. Springer, Berlin, Heidelberg (2013)
- Tlig, M., Buffet, O., Simonin, O.: Stop-free strategies for traffic networks: Decentralized on-line optimization. In: ECAI 2014, pp. 1191–1196. IOS Press, Amsterdam (2014)
- Zhu, Z., Adouane, L., Quilliot, A.: Hierarchical control for trajectory-based intelligent navigation in urban adjacent intersections. In: 2021 IEEE International Intelligent Transportation Systems Conference (ITSC), pp. 948–954. IEEE, Piscataway, NJ (2021)
- Zhu, Z., Adouane, L., Quilliot, A.: Intelligent traffic based on hybrid control policy of connected autonomous vehicles in multiple unsignalized intersections. In: 2021 IEEE SmartWorld, Smart City Innovation (SCI), pp. 416–424. IEEE, Piscataway, NJ (2021)
- He, Z., Qi, G., Lu, L., Chen, Y.: Network-wide identification of turn-level intersection congestion using only low-frequency probe vehicle data. *Transp. Res. Part C: Emerg. Technol.* 108, 320–339 (2019)

42. Li, L., Chen, X.M.: Vehicle headway modeling and its inferences in macroscopic/microscopic traffic flow theory: a survey. *Transp. Res. Part C: Emerg. Technol.* 76, 170–188 (2017)
43. Geroliminis, N., Daganzo, C.F.: Existence of urban-scale macroscopic fundamental diagrams: some experimental findings. *Transp. Res. Part B: Methodol.* 42(9), 759–770 (2008)
44. Keyvan Ekbatani, M., Kouvelas, A., Papamichail, I., Papageorgiou, M.: Exploiting the fundamental diagram of urban networks for feedback-based gating. *Transp. Res. Part B: Methodol.* 46(10), 1393–1403 (2012)
45. Mahmassani, H.S., Hou, T., Saberi, M.: Connecting networkwide travel time reliability and the network fundamental diagram of traffic flow. *Transp. Res. Rec.* 2391(1), 80–91 (2013)
46. Turner, S.M., Eisele, W.L., Benz, R.J., Holdener, D.J.: *Travel Time Data Collection Handbook*. Federal Highway Administration, Washington, D.C. (1998)
47. Knoop, V., Hoogendoorn, S.P., van Zuylen, H.: Empirical differences between time mean speed and space mean speed. In: *Traffic and Granular Flow'07*, pp. 351–356. Springer, Berlin, Heidelberg (2009)
48. Greenshields, B., Bibbins, J., Channing, W., Miller, H.: *A Study of Traffic Capacity*. Vol. 1935, Highway Research Board, Washington, D.C. (1935)
49. Lakhal, N.M.B., Adouane, L., Nasri, O., Slama, J.B.H.: Interval-based/data-driven risk management for intelligent vehicles: application to an adaptive cruise control system. In: 2019 IEEE Intelligent Vehicles Symposium (IV), pp. 239–244. IEEE, Piscataway, NJ (2019)
50. Lakhal, N.M.B., Nasri, O., Adouane, L., Slama, J.B.H.: Reliable modeling for safe navigation of intelligent vehicles: analysis of first and second order set-membership TTC. In: *Proceedings of the 17th International Conference on Informatics in Control, Automation and Robotics - Volume 1: ICINCO*, pp. 545–552. SciTePress, Paris (2020)
51. Hult, R., Campos, G.R., Falcone, P., Wymeersch, H.: An approximate solution to the optimal coordination problem for autonomous vehicles at intersections. In: 2015 American Control Conference (ACC), pp. 763–768. IEEE, Piscataway, NJ (2015)
52. Kühne, F., Gomes, J., Fetter, W.: Mobile robot trajectory tracking using model predictive control. *IEEE LARS*, pp. 1–7. IEEE, Piscataway, NJ (2005)
53. Wang, Y., Cai, P., Lu, G.: Cooperative autonomous traffic organization method for connected automated vehicles in multi-intersection road networks. *Transp. Res. Part C: Emerg. Technol.* 111, 458–476 (2020)

How to cite this article: Zhu, Z., Adouane, L., Quilliot, A.: Decentralised CAVs based on micro–macro flow control (MiMaFC) strategy for multi-intersection traffic network. *IET Intell. Transp. Syst.* 17, 499–517 (2023). <https://doi.org/10.1049/itr2.12276>